

AIR MOVEMENT & VENTILATION CONTROL WITHIN BUILDINGS

12th AIVC Conference, Ottawa, Canada  
24-27 September, 1991

POSTER 54

THEORETICAL AND EXPERIMENTAL ANALYSIS  
OF DIFFERENT VENTILATION STRATEGIES IN A TEST ROOM

N.Cardinale, G.V.Fracastoro, M.Mantegna\*, E.Nino\*\*

\* Dipartimento di Energetica - Politecnico di Torino  
Corso Duca degli Abruzzi 24, - 10100 TORINO (Italy)

\*\*Dipartimento di Ingegneria e Fisica dell' Ambiente  
Universita' della Basilicata  
Via Nazario Sauro, 85- 85100 POTENZA (Italy)

## ABSTRACT

The paper presents an original computer code for the analysis of contaminant diffusion in rooms developed at the Politecnico di Torino and its experimental validation by means of a test facility located at the University of Basilicata (Potenza). The velocity fields in isothermal conditions, together with local ages of the air, have been analysed and compared, with different ventilation strategies and number of air changes.

### Introduction

There is a growing interest on the topic of contaminant diffusion both outdoor and indoors. Indoors, the study of this type of problem has consequences both on the hygienic and on safety sides (e.g., for the analysis of explosion risks related to gas leaks).

There are many available computer codes in this area (see, e.g., Liddament, 1991), but there is still a need for further research, mainly for two reasons: firstly, these computer codes have often been created and validated for purposes different from the one considered herein; secondly, commercial codes have a wide but fixed range of possible outputs, which not always include the most interesting parameters in the ventilation studies, such as ventilation efficiency, local ages of the air, etc.

The aim of this paper is to present a new computer code, which was explicitly created for the study of the fluid dynamic field and contaminant dispersion in a room. At this preliminary stage, the concentration field is not yet computed. Therefore the programme has been experimentally validated only on the basis of velocity values.

The experimental validation has been conducted using the Controlled Ventilation Chamber of the University of Basilicata, whose description was the aim of a previous paper (Fracastoro and Nino, 1990)

Results are presented both in terms of the velocity field (although the experimental results only yield nondirectional data) and local ages of the air.

### Description of the calculation procedure

The calculation method hereby described is a method which solves the fluid dynamic field for two-dimensional problems in isothermal conditions. The domain is discretized in square cells, and to each cell the continuity equation and Navier-Stokes equations are applied.

The first set of equations is the local formulation of the continuity law:

$$\frac{\delta(\rho u)}{\delta x} + \frac{\delta(\rho v)}{\delta y} = 0$$

where  $u$  and  $v$  are the horizontal and vertical components of velocity, and  $\rho$  is the density. For incompressible fluids the equation above is linear in  $u$  and  $v$ .

The second and third sets of equations are the scalar form in  $x$  and  $y$  of the vectorial Navier-Stokes equation in local formulation (dynamic equilibrium):

$$\rho \left( u \frac{\delta u}{\delta x} + v \frac{\delta u}{\delta y} \right) = \mu \left( \frac{\delta^2 u}{\delta x^2} + \frac{\delta^2 u}{\delta y^2} \right)$$

$$\rho \left( u \frac{\delta v}{\delta x} + v \frac{\delta v}{\delta y} + F \right) = \mu \left( \frac{\delta^2 v}{\delta x^2} + \frac{\delta^2 v}{\delta y^2} \right)$$

where  $F$  is the intensity of the force field (gravitational field) and  $\mu$  is the dynamic viscosity of the fluid. The first step for the solution of the problem, due to the low velocities involved, was to assume a hydrostatic pressure distribution.

The equation of continuity was then applied in order to make the first estimate of the scalar velocity field.

It is well known that there are two velocity potentials  $\Phi$  and  $\phi$ , whose equipotential lines are mutually orthogonal. These equipotential lines may be easily determined for some simple configurations, such as the flow over a flat indefinite surface (for which the  $\Phi = \text{constant}$  lines are parallel to the surface). Once these equipotential lines are known for a simple domain, they may be determined for more complex domain using the theory of conformal mapping (Spiegel, 1964). This theory, illustrated in texts of complex numerical calculus, has already been usefully employed in engineering problems such as air flow around wing profiles. The transformation of a simple domain contour into a complex one (such as a polygonal contour) may be performed thanks to the Schwartz-Christoffel theory (Mantegna, 1991).

During the transformation the equipotential lines are also transformed, but due to the propriety of isogonality of conformal mapping, the new equipotential lines are still mutually orthogonal, except in the singular points of the contour. The decomposition of the domain into regions for which application of conformal mapping is possible, and the subsequent juxtaposition of the velocity fields of the various regions allows to obtain the complete velocity field for the test chamber. Once the equipotential lines in the new domain are known, the velocity field satisfying the continuity equation may be

deduced by derivation. In general this field will not, however, satisfy the Navier-Stokes equations.

This approach is different from the procedure ordinarily used in other types of solvers, such as the SIMPLE solver (Patankar, 1980). In fact, SIMPLE obtains the velocity field solving alternately the continuity equation and the dynamic balance equation, while in our case the equation of continuity is solved once for all through conformal mapping.

Now, an iterative method is needed to obtain a dynamically better balanced solution, while maintaining the mass balance. A dynamically better balanced solution means a solution in which the residuals at the right side of Navier-Stokes equation are as close as possible to zero. The idea was to make use of a generalized version of Cross's method, widely used for plant applications (Monte, 1987). Fig. 1 shows a fragment of the square cells into which the domain has been discretized. The fictitious "elementary vortex" superimposed to the motion field in the cell will keep the mass balance, eventually causing a partial deviation of the flow. By choosing in a suitable way the intensity of such vortex, the global dynamic unbalancement may be reduced.

In such a way, the two scalar velocities sets are substituted by two new sets of unknowns: vortex intensities and pressures. It should be stressed that the algebraic equations are second degree equations only in the vortex unknowns, while they are linear in the pressures: this makes clear why it is convenient to deal differently with these two sets of unknowns. Also the SIMPLE method adopts this procedure, but the correction equations for pressure are obtained from the continuity equation, while the present method does not make any more use of mass balance equations. However, the pressure values may be corrected as if the most recent velocity values were constant.

The exact process of constructing vortex- and pressure correction equations involves a lot of details and is explained in another paper (Mantegna, 1991). Basically, two families of equations are obtained by summing and subtracting Navier-Stokes equations for horizontal and vertical balance.

Whenever no boundary condition on pressure is assigned at the walls, it may be assumed that the pressure gradient orthogonal to the wall is zero (This is equivalent to neglect the velocity component orthogonal to the wall itself).

The corrected pressure field is then substituted into another set of equations, namely the velocity correction equations (Mantegna, 1991).

For the solution of the velocity correction equations, the pressures are considered to be constant, and their best estimates, corresponding to underrelaxation of the pressure correction equations, are introduced. Also the velocities are considered to be constant, and the most recent available value is adopted: but an unknown set of

vortex intensities is superimposed to the velocity set for each cell.

By the way, there is no need to solve accurately at this stage the velocity correction equations, because the pressure values adopted are only estimates. Due to the fact that the velocity correction equations are higher than first degree equations, these can be solved by means of their gradients. In each equation, only at most 9 elementary vortex intensities (those affecting the considered cell) appear. Thus, the matrix of coefficients will be "sparse", and suitable iterative techniques may be used to solve it.

The underrelaxed values of the elementary vortex intensities are then used to correct the velocity field in each cell.

The iterative method proceeds solving alternatively the correction equations for pressure and velocity until convergence is attained. The right sides of the dynamic equilibrium equations (equal to zero for the exact solution) are taken as indicators of convergence.

When the velocities are sufficiently high the Reynolds number will surpass the maximum stability limit of laminar flow, and the regime will become turbulent. In this case the dynamic equilibrium equations valid for laminar flow are modified following the Boussinesq hypothesis, by introducing the concept of turbulent viscosity  $\mu_t$ . Since turbulent viscosity is no longer a property of the fluid, the Boussinesq hypothesis has to be integrated by a "turbulence model" in order to calculate cell by cell the values of turbulent viscosity. A large number of turbulence models have been proposed, starting from Prandtl model. Nowadays, the prevailing method is the so called k- $\epsilon$  method, proposed by Launder and Spalding (1972 and 1973), and subsequently modified by other authors. No model up to know is able to reproduce all the experimental results obtained on turbulence. For each type of problem there is a technique which proves itself more suitable than others.

For the case considered in this paper, one of the most important limitations is the low Reynolds number, sometimes even falling into the transition region. For this reason the k- $\epsilon$  turbulence model as modified by Jones and Launder (1972) was adopted. The equation of transport for k assumes the following form:

$$\rho \left( \frac{\delta k}{\delta t} + u \frac{\delta k}{\delta x} + v \frac{\delta k}{\delta y} \right) = \frac{\delta}{\delta x} \left( \mu + \frac{\mu_t}{\sigma} \right) \frac{\delta k}{\delta x} + \frac{\delta}{\delta y} \left( \mu + \frac{\mu_t}{\sigma} \right) \frac{\delta k}{\delta y} + \frac{P_k}{k} + \frac{G_k}{k} - \rho \epsilon + D$$

where  $P_k$  is the shear production of turbulent kinetic energy,  $G_k$  is the buoyancy production of turbulent kine-

tic energy and  $D$  is the source term,  $\sigma_k$  is the turbulent Prandtl number for  $K$ . (Henkes, Van der Vlugt and Hoogendoorn, 1991).

On the other side the equation of transport for  $\epsilon$  takes the form:

$$\rho \left( \frac{\delta \epsilon}{\delta t} + u \frac{\delta \epsilon}{\delta x} + v \frac{\delta \epsilon}{\delta y} \right) = \frac{\delta}{\delta x} \left( \mu + \frac{\mu_t}{\sigma_\epsilon} \right) \frac{\delta \epsilon}{\delta x} + \frac{\delta}{\delta y} \left( \mu + \frac{\mu_t}{\sigma_\epsilon} \right) \frac{\delta \epsilon}{\delta y} + \left( c_1 f_1 (P + c_3 G) + c_2 \rho f_2 \epsilon \right) - E$$

where  $E$  is the source term,  $\sigma_\epsilon$  is the turbulent Prandtl number for  $\epsilon$ , while  $c_1$ ,  $c_2$ ,  $c_3$ ,  $f_1$  and  $f_2$  are constants of method (Henkes, Van der Vlugt and Hoogendoorn, 1991).

The transport equations for the turbulent quantities are formally similar to the dynamic equilibrium equations, and may be solved adopting an identical solution technique.

#### Input-output of the programme AIR

The ordinary commercial codes, being totally general, need definition of the domain case by case. On the opposite, this programme is already prearranged for a rectangular domain with a variable number of immission/extraction grilles. Then we only type in the geometrical features of the room and of immission and exhaust grilles which include the number of these.

Other input data are the discretization parameters and in particular the number of cells for each side. If there are  $n$  grilles, we need to type in the module and direction of velocity for  $n-1$  grilles and only the direction for the last grille because the module will be derived from the continuity equation.

The output data (both numerical and graphical) are the pressure, the velocity and the local mean age of air in each cell and the room mean age of air. The room mean age of air is an indicator providing a global idea of the ventilation efficiency of a room. In particular we define the local age of air as the time required by the air to move from the immission grille to a generic point in the room.

The local mean age of air in a point is the arithmetic mean of the different local ages of the air. In practice it may be calculated as the average of the local ages of the adjacent nodes weighed according to the incoming flow rates. Since air density may be considered constant the average may be obtained using as weights the local velocities.

The room mean age is the arithmetic mean of the local

mean ages in each point of the room. Since the velocity field is continuous the arithmetic mean is calculated as the volume integral of the local mean age, extended to the whole room and divided by the room volume.

### The experimental facility

A concise description of the main features of the Controlled Ventilation Chamber (CVC) follows:

- Size : 3.00 (x - extensible to 4.20) x 2.40 (y) x 2.40 (z - height)

- Possible ventilation strategies: balanced, immission or extraction. Four positions of grilles on walls y-z

- Special features: one transparent x-z wall

- Range of air changes per hour: 0 to 10 ach

- Instrumentation:

Two-cell Gas Analyzer ( $\text{SF}_6$  and  $\text{NO}_2$ ), range 0 to 200 ppm

Six non-directional hot film anemometers, range 0 to 0.5 m/s

Flowmeter for the measurement of air flow rate to the CVC

An automatic system for air sampling at six different locations

An automatic system for moving the sensors around the chamber

### Measurement campaigns

The CVC has already been used for many experimental campaigns which have helped to improve the performance of the instrumentation and to define its accuracy.

These include pressurisation tests, decay tests with perfect mixing, velocity at the outlets of the immission grilles, measurement of ventilation efficiencies during decay, buildup, and steady-state sequences (see, e.g., Cafaro et al., 1991).

Since it has been observed (Cafaro et al., 1991) that not only the fluid dynamic field influences the concentration field, but also the opposite thing happens (i.e., the contaminant concentration affects the velocity field), the comparison has been made only on the grounds of velocity fields, without any contaminant in the room.

### Comparison between experimental and theoretical results

Many different ventilation strategies (as for grilles positioning and number of air changes) may be simulated experimentally (see Figure 2), but the comparison between theoretical and experimental results presented in this paper refers only to strategies B and C:

B) Air immission from a lower grille and extraction from the higher grille placed on the opposite wall

C) Air immission from a lower grille and extraction from

the higher wall on the same side

The experimental velocity data are known at five points simultaneously (because one of the six anemometers was excluded due to its higher range - 0 to 5 m/s). Each value is the result of 50 consecutive measurements lasting about 1'. In order to improve the detail in the knowledge of the velocity field, the five measurement points were moved along the vertical symmetry plane of the CVC.

The theoretical data are known at each cell. There was a total number of 720 cells for the cases presented. Results are compared in terms of velocity moduli only, because the CVC is provided with non-directional anemometers.

Two cases have been compared: Strategy B with 3 ach (case B3) and strategy C with 3 ach (case C3).

For case B3 a total number of 210 measurement points is available. In the area close to the inlet grille (Figures 3 and 4), there is a moderately good agreement for both  $x = 270$  cm and  $x = 280$  cm axes, especially in the lower zone. Close to the ceiling there is a clear underestimate of the code. In general, the experimental values are higher than the calculated ones, and in some cases the measured value also exceeds the air velocity at the grille. This is probably due to the actual non-uniformity of inlet velocity profiles.

Proceeding towards the exhaust, in the central area (Figures 5 and 6) there is a clear agreement between calculated and measured results in the lower zone and somehow less good agreement in the upper zone. On the opposite, while the calculations clearly show only one vortex at mid height, the measurements give prominence of a double vortex, the first being just above the inlet grille, and the second at about the same height as the computed one.

Close to the exhaust grille (Fig 7 and 8), there is little resemblance between calculated and measured velocity profiles.

For case C3 there are only 90 experimental data available, and the comparison is shown in figures 9, 10 and following. Close to the inlet/outlet grilles, the experimental data give evidence of a strong air flow closest to the grilles, increasing with height and decreasing with the distance from the grilles. All the region seems to be interested by the phenomenon, while the calculations show a marked effect at the grilles height, leaving the intermediate area practically undisturbed.

In the central area, the results are much more promising, both for the qualitative agreement and the actual values of velocity. Finally, close to the wall opposite to the grilles, there is again little agreement between experimental and theoretical results.



## Future developments and conclusions

The results presented in this paper are still preliminary and require a more careful validation than it was possible to do up to this moment.

In some cases the results are encouraging, in others the model AIR seems to simplify to some extent the actual physical phenomenon. However, the work done has helped both for a better understanding of the phenomena and also to improve the experimental techniques.

The code will soon calculate also the concentration field for contaminants and a better estimate of  $k$ - $\epsilon$  parameters will also be available. The possibility of allowing variable size cells will also be taken into consideration.

On the experimental side it will soon be possible to make experiments with non-uniform temperature field. There are also solid hopes to make use in a short time of more powerful techniques, like laser-doppler anemometry, to define the velocity field.

## Acknowledgements

The authors wish to thank Franco Mariniello for his skillfull help in the execution of measurements.

## References

Cafaro, E., Fracastoro, G.V., Nino, E., Perino, M., Analisi teorico-sperimentale della diffusione degli inquinanti negli ambienti confinati. Convegno ATI, Gaeta, 1991.

Fracastoro, G.V., Nino, E., and Coretti, G., The Ventilation Chamber of the University of Basilicata, Proc. 11th AIVC Conference, Belgirate (Italy), 1990.

Fracastoro, G.V., Nino, E., La Camera a Ventilazione Controllata dell'Università della Basilicata, Convegno AICARR, Roma, 18-19 Aprile 1991.

Henkes R.A.W.M, Van der Vlugt F.F., Hoogendoorn C.J, Natural convection flow in a square cavity calculated with low-Reynolds number turbulence models, Int.J Heat Mass Transfer, vol.34, n.2, 377-388, 1991

Jones W.P., Launder B.E, The prediction of laminarization with a two-equation model of turbulence, Int.J Heat Mass Transfer, 15, 301-314, 1972

Launder B.E., Spalding D.B, Mathematical models of turbulencs, Academic Press, London, 1972

Lauder B.E, Spalding D.B, The Numerical computation of Turbulent Flows, Comp. Meth.in App. Mech. and Engineering, 3, 269-289, 1974

Liddament, M.W., A Review of Building Air Flow Simulation. AIVC, Technical Note 33, March 1991.

Mantegna, M., Un metodo di calcolo della ventilazione negli ambienti (in press), 1991

Monte A., Impianti meccanici, ed.Cortina, 1987

Patankar S.V, Numerical Heat Transfer and Fluid Flow, Hemisphere Publishing Co, 1980

Spiegel M.R, Theory and Problems of Complex Variables, Schaum Publishing Co., New York, 1964

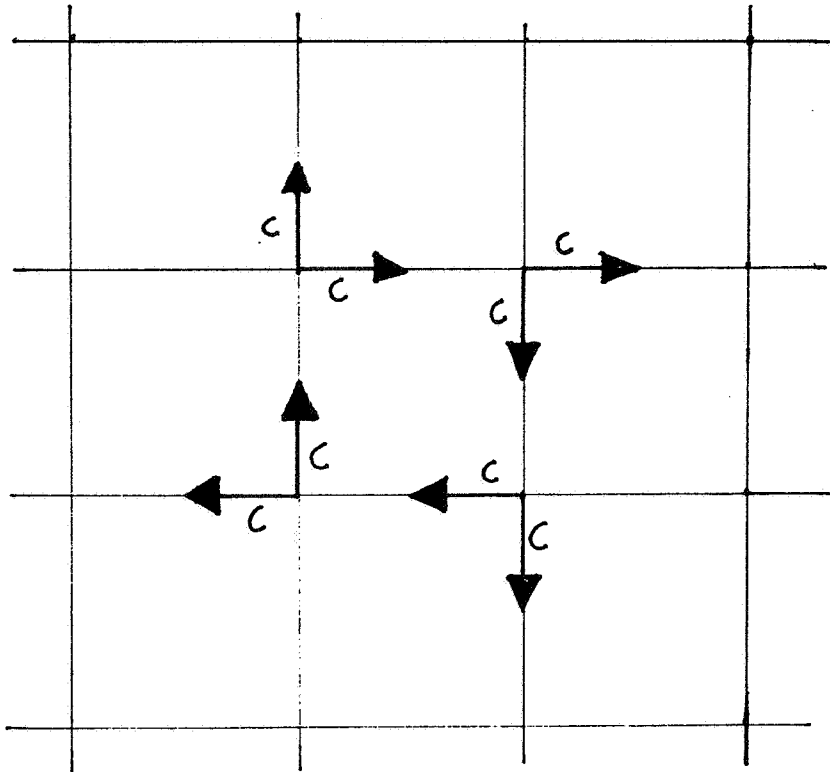


fig.1 - Fragment of the square cells of the domain with the "elementary vortex"

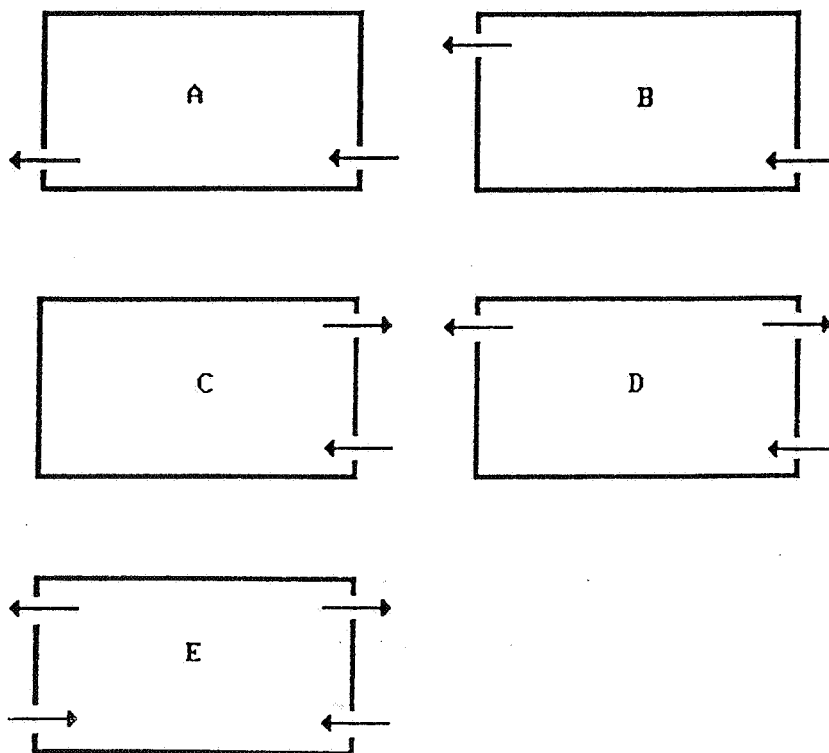


fig.2 - Ventilation strategies

### B3 - Experimental velocities

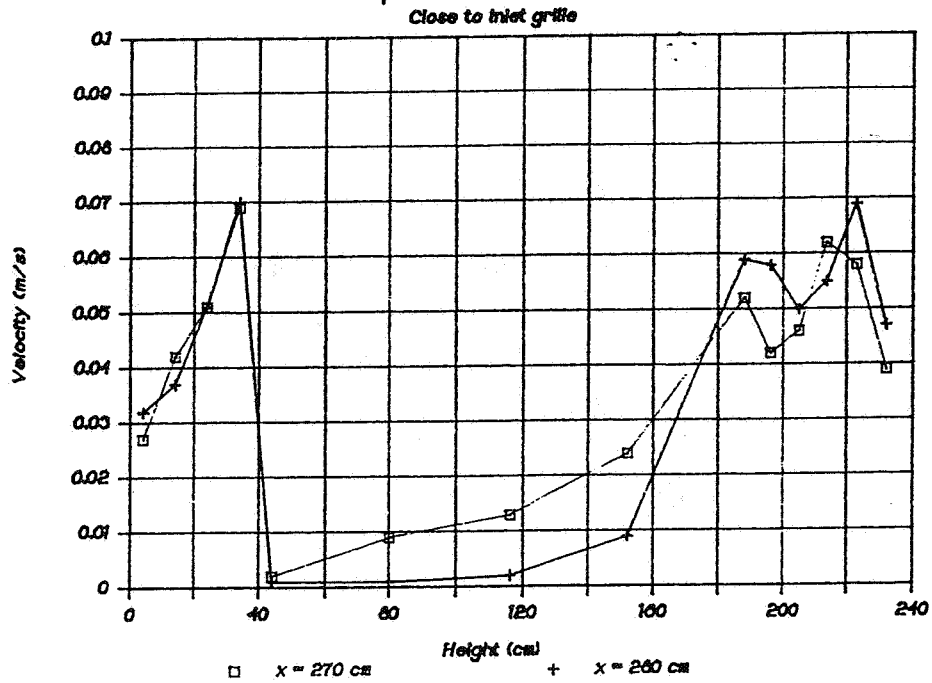


fig.3 - Experimental velocities close to inlet grille for strategy B with 3 ach

### B3 - Calculated velocities

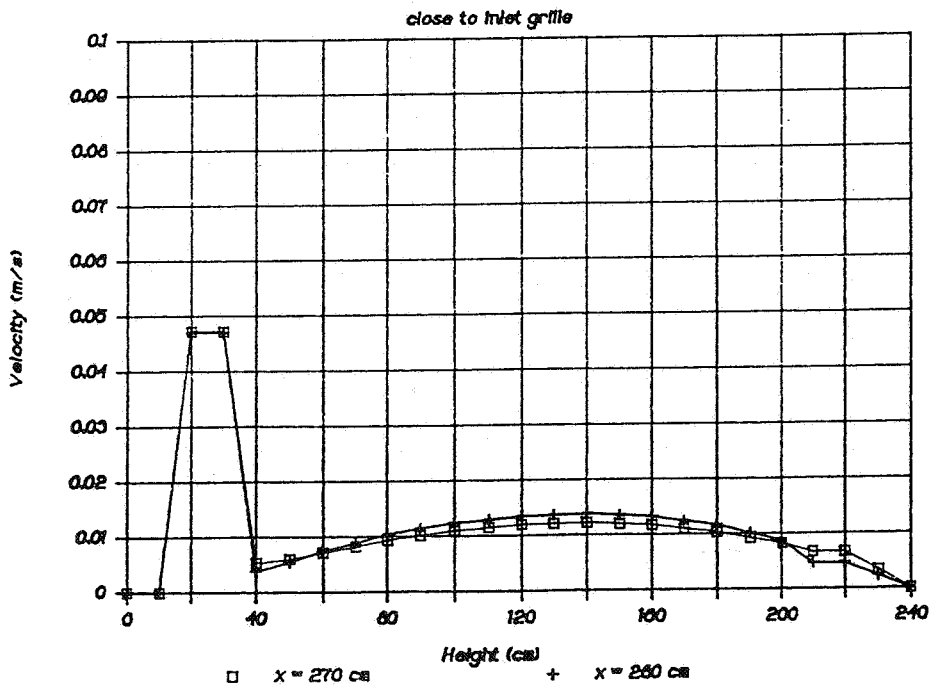


fig.4 - Calculated velocities close to inlet grille for strategy B with 3 ach

### B3 - Experimental velocities in the central area

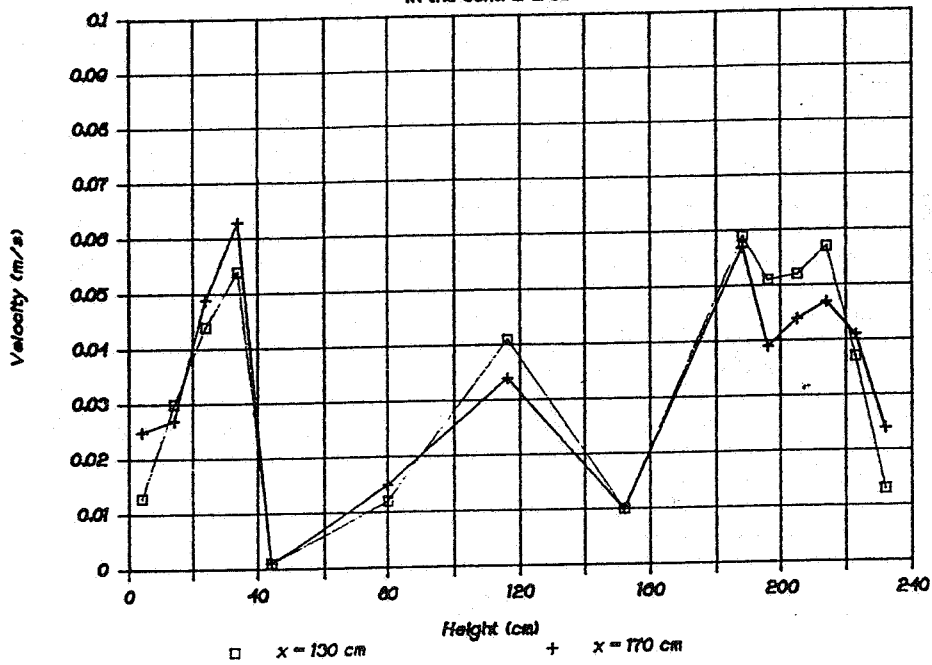


fig.5 - Experimental velocities in the central area for strategy B with 3 ach

### B3 - Calculated velocities in the central area

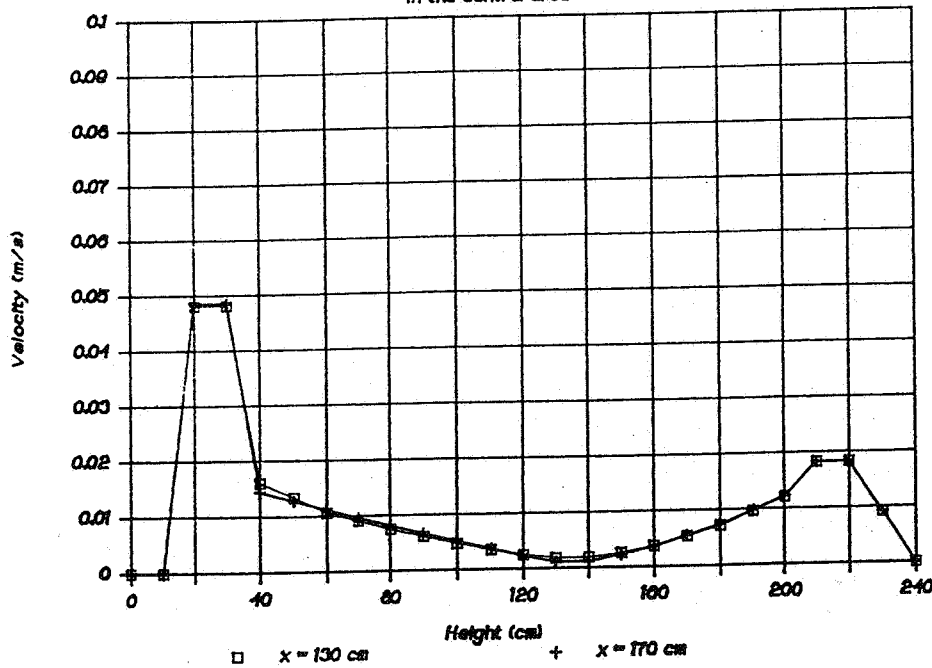


fig.6 - Calculated velocities in the central area for strategy B with 3 ach

### B3 - Experimental velocities

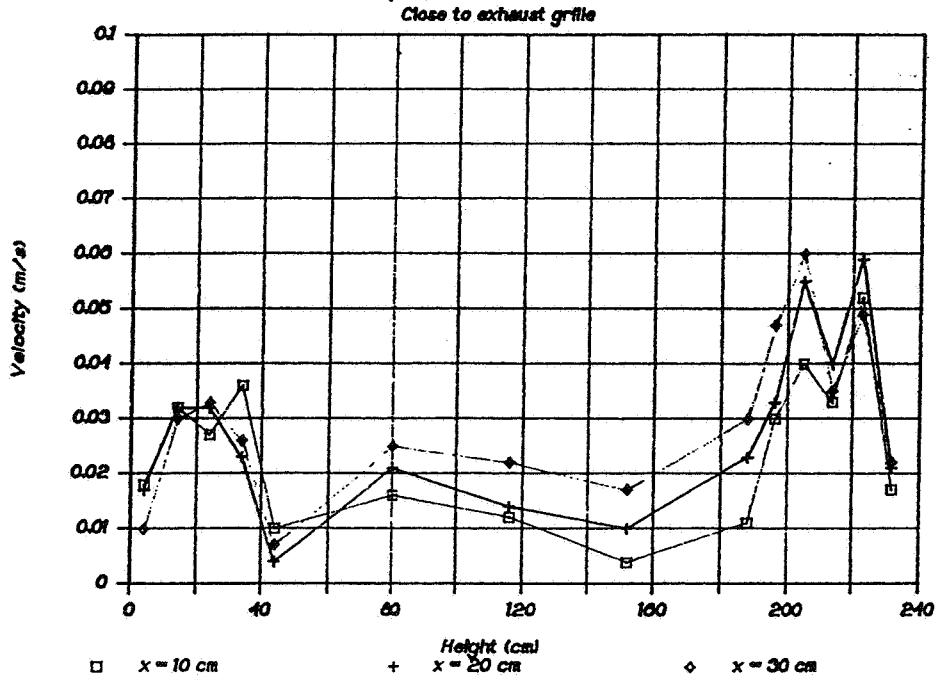


fig.7 - Experimental velocities close to exhaust grille for strategy B with 3 ach

### B3 - Calculated velocities

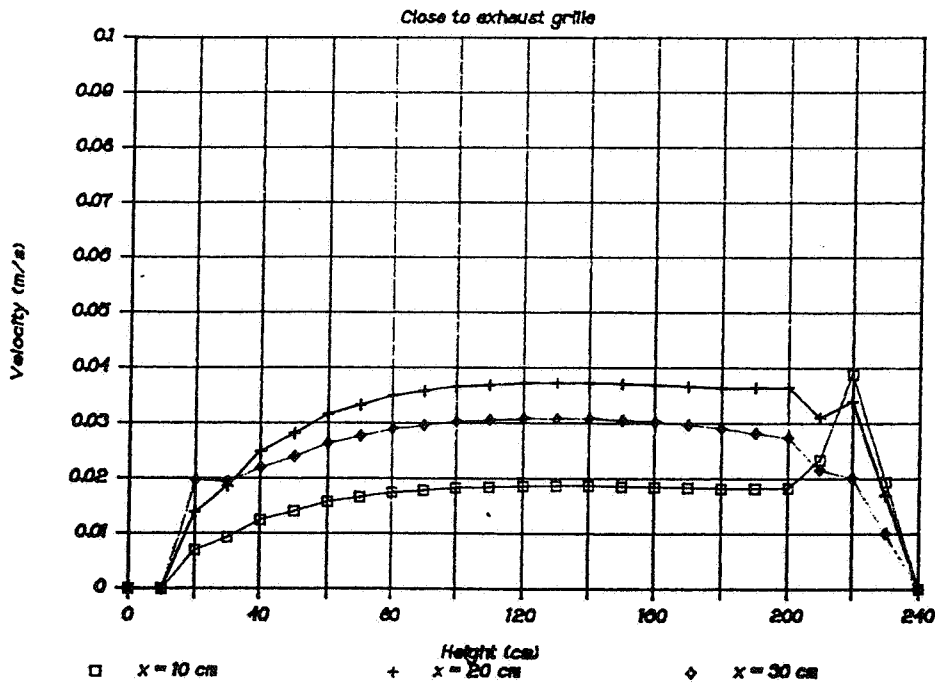


fig.8 - Calculated velocities close to exhaust grille for strategy B with 3 ach

### C3 - Experimental velocities

close to the inlet/outlet

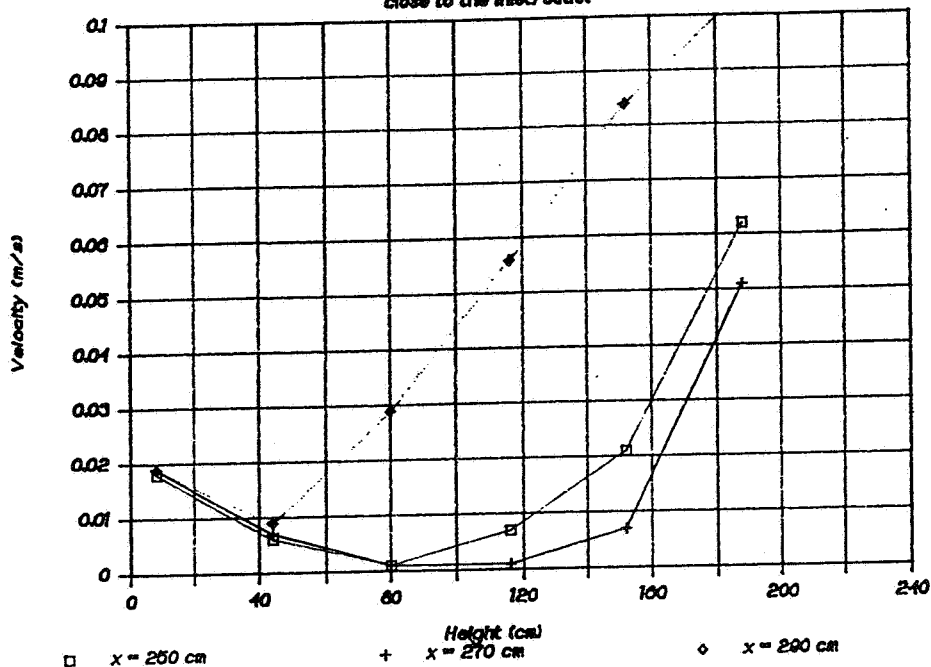


fig.9 - Experimental velocities close to inlet/outlet grilles for strategy C with 3 ach

### C3 - Calculated velocities

close to inlet/outlet grilles

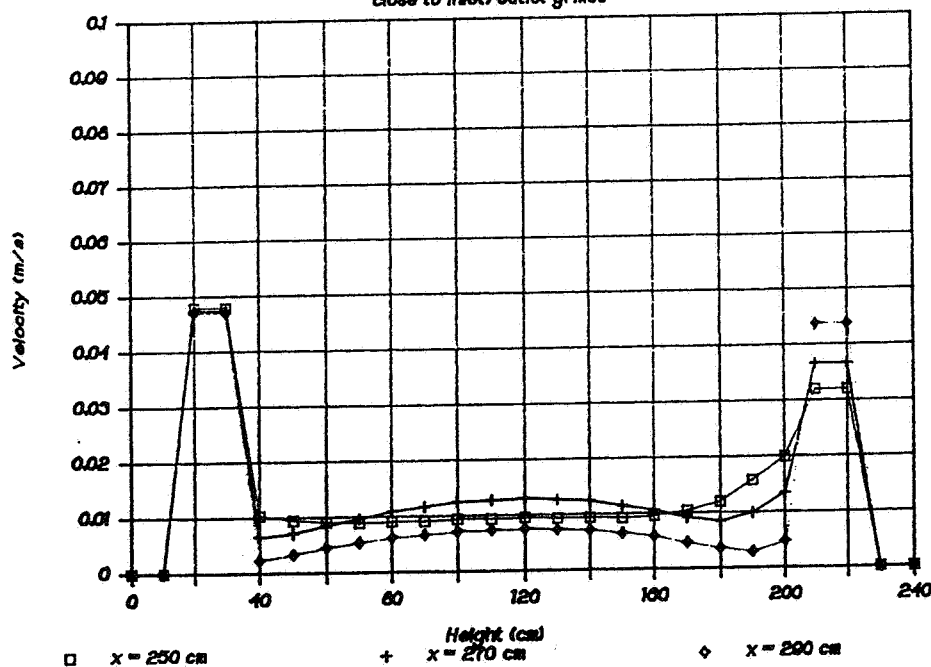


fig.10- Calculated velocities close to inlet/outlet grilles for strategy C with 3 ach

### C3 - Experimental velocities in the central area

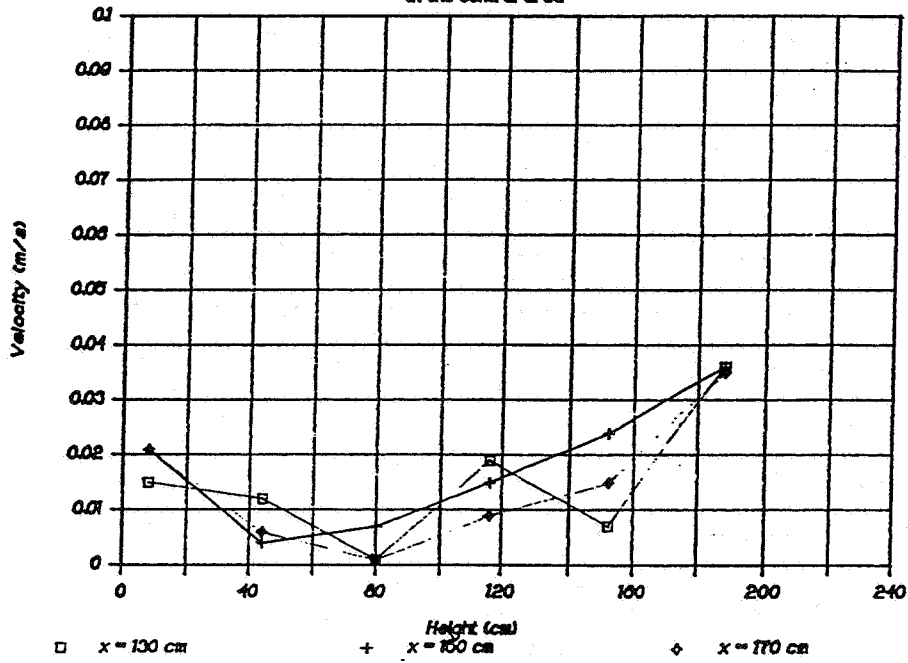


fig.11- Experimental velocities in the central area for strategy C with 3 ach

### C3 - Calculated velocities in the central area

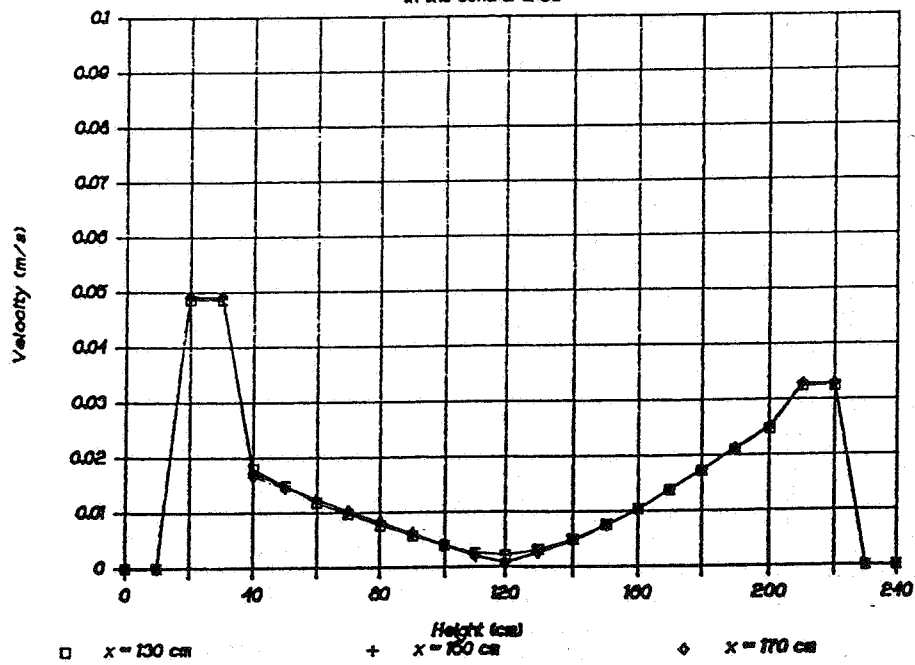


fig.12- Calculated velocities in the central area for strategy C with 3 ach



### C3 - Experimental velocities opposite to inlet/outlet grilles

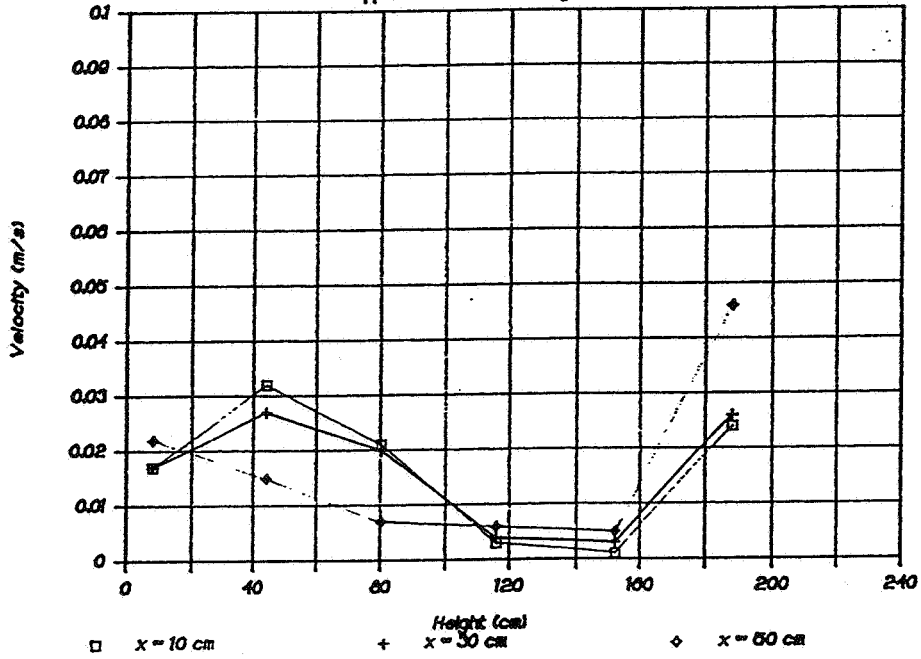


fig.13- Experimental velocities opposite to inlet/outlet grilles for strategy C with 3 ach

### C3 - Calculated velocities opposite to inlet/outlet grilles

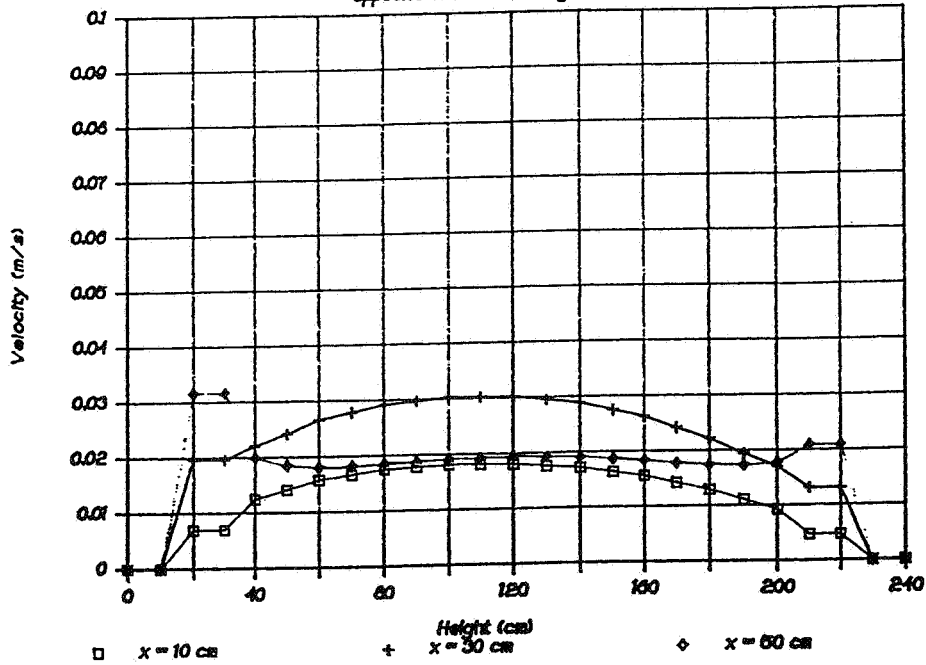


fig.14- Calculated velocities opposite to inlet/outlet grilles for strategy C with 3 ach